UNCLASSIFIED 14 DEC 1989

AD-A216 319

REPORT DOCUMENTATION PAGE

Form Approved OMB No 0704-0188

1a REPORT SECURITY CLASSIFICATION UNCLASSIFIED	1b RESTRICTIVE MARKINGS
2a SECURITY CLASSIFICATION AUTHORITY	3 DISTRIBUTION/AVAILABILITY OF REPORT Approved for public release; distribution is unlimited.
2b DECLASSIFICATION / DOWNGRADING SCHEDULE	
4 PERFORMING ORGANIZATION REPORT NUMBER(S)	5 MONITORING ORGANIZATION REPORT NUMBER(S) AFOSR-TR- 89-1817
6a NAME OF PERFORMING ORGANIZATION California Institute of Technology 6b OFFICE SYMBOL (If applicable)	7a NAME OF MONITORING ORGANIZATION AFOSR/NC
6c ADDRESS (City, State, and ZIP Code) Pasadena, CA 91125	7b ADDRESS (City, State, and ZIP Code) Building 410, Bolling AFB DC 20332-6448
8a NAME OF FUNDING/SPONSORING ORGANIZATION AFOSR 8b OFFICE SYMBOL (If applicable) NC	9 PROCUREMENT INSTRUMENT IDENTIFICATION NUMBER AFOSR-87-0071
8c ADDRESS (City, State, and ZIP Code) Building 410, Bolling AFB DC 20332-6448	10 SOURCE OF FUNDING NUMBERS PROGRAM ELEMENT NO 61102F; PROJECT NO. 2303; TASK NO B1; WORK UNIT ACCESSION NO

11. TITLE (Include Security Classification)
(U) ULTRAFAST CHEMICAL DYNAMICS OF REACTIONS IN BEAMS

12. PERSONAL AUTHOR(S)
Ahmed H. Zewail - principal investigator

13a. TYPE OF REPORT	13b. TIME COVERED	14. DATE OF REPORT (Year, Month, Day)	15. PAGE COUNT
FINAL REPORT	FROM 1Nov.86 TO 31Oct.89		16

16. SUPPLEMENTARY NOTATION

17 COSATI CODES			18. SUBJECT TERMS (Continue on reverse if necessary and identify by block number)
FIELD	GROUP	SUB-GROUP	femtochemistry-ultrafast dynamics-chemical bond breakage-real time-transition state-high resolution lasers-unimolecular reactions-femtosecond time scale-reaction dynamics. Reaction Kin

19. ABSTRACT (Continue on reverse if necessary and identify by block number)

The purpose of this research was to initiate the field of femtochemistry by interfacing state-of-the art femtosecond laser systems to a beam system. This plan allowed us to study, for the first time, the ultrafast dynamics of chemical bond breakage in reactions under collisionless conditions (beams). The success of these experiments, which view the process directly in real-time, created a wealth of information on the nature of the transition state and the resultant internal states distribution. A summary of the achievements together with the list publications is presented in this report. Photochemical Reactions

90 01 04 124

20. DISTRIBUTION/AVAILABILITY OF ABSTRACT ☐ UNCLASSIFIED/UNLIMITED ☐ SAME AS RPT ☐ DTIC USERS	21 ABSTRACT SECURITY CLASSIFICATION UNCLASSIFIED
22a NAME OF RESPONSIBLE INDIVIDUAL L P DAVIS, MAJOR, USAF	22b TELEPHONE (Include Area Code) (202) 767-4963; 22c OFFICE SYMBOL AFOSR/NC

DD Form 1473, JUN 86 Previous editions are obsolete. SECURITY CLASSIFICATION OF THIS PAGE

UNCLASSIFIED

Final Report

AFOSR-87-0071
1 November 1986 - 31 October 1989

ULTRAFAST CHEMICAL DYNAMICS OF REACTIONS IN BEAMS

SUMMARY OF WORK ACCOMPLISHED

In this report we highlight our achievements (and failures) of the work supported by this grant by summarizing the findings presented in some twenty publications of the Caltech group and to the citations given in every section.

A. The Development of the Probing Method

To study reactions on the femtosecond time scale, we needed a sensitive probe of the transition-state(s) region. The so-called femtosecond transition-state spectroscopy FTS method [M. Dantus, M. Rosker, and A. Zewail, J. Chem. Phys. 87, 2395 (1987)] was developed to monitor photodissociation reactions with a distance resolution of ≤ 0.1 Å. Since the recoil velocity of fragments is typically 1 km s^{-1}, the current state of the art in femtosecond technology (6 fs duration) allows one to view the PES with a distance resolution of ~ 0.06 Å.

FTS is a pump-probe method that allows us to obtain snapshots of reactions while fragments are separating, or encountering each other. If ultrashort pulses are employed, the sensitivity of the detection is enhanced by a factor of 10^4-10^6 when compared with time-integrated, steady-state, experiments. Essentially all molecules traversing the transition-states can be detected, and this is a key feature of FTS. The difficulty, however, comes in generating pulses and in developing the techniques for observing changes on the femtosecond time scale.

The FTS signal recorded is some measure of the absorption by the fragment of the probe pulse at wavelength λ_2 as a function of the time-delay τ between pump and probe. This could be accomplished, for instance, by measuring the change in the transmission of the probe. Since the experiment would not be background free, far better sensitivity can be obtained through, for instance, the detection of the laser-induced fluorescence (LIF), or the multiphoton ionization (MPI) generated by the probe. Typically, we measure the FTS signal when λ_2 is tuned to the absorption wavelength of the free fragment, $\lambda_{2\infty}$ (where ∞ denotes that $R \rightarrow \infty$), and at a number of wavelengths absorbed by the transition-states, λ_2^* (where * denotes the transition-

state region of R). Then a surface of measurements $A(t; \lambda_{2(a)}^*, \lambda_{2(b)}^*, ..., \lambda_{2\infty})$ is constructed. This surface is related to the dynamics and to the PES of the reaction, as we will discuss below. The experiments are then repeated for different pump wavelengths (λ_1)--see Fig. 1.

B. Unimolecular Dissociation Reactions

In the simplest FTS experiment (clocking), the probe is centered at an absorption of one of the free fragments. In this case, the absorption of the probe will be initially negligible, and will only become substantial when the fragments achieve large internuclear distance and are therefore (essentially) non-interacting. The delay at which the probe absorption "turns on," $\tau_{1/2}$, is therefore a measurement of the time required for complete (or nearly complete) internuclear separation. In other words, FTS provides a "clock" of the time required to break the bond.

The experiment can be pictured simply as a measure of the femtosecond "time-of-flight" on the excited-state PES from the initially excited configuration at R_0 to the free fragment configuration, where the probe opens a "window" on the PES. If the experiment is performed for various probe spectral widths, then additional information on the asymptotic shape of the potential can be obtained. Additionally, the clocking experiment offers significant practical advantages which have been discussed in details elsewhere (see publications). Such clocking experiments have been performed on the dissociation reaction of ICN.

$$ICN^* \rightarrow [\, I \cdots CN \,]^{\ddagger *} \rightarrow I + CN,$$

and provide $\tau_{1/2} = 205 \pm 30$ fs (see Fig. 2).

FTS experiments can also be made by tuning λ_2 away from the transition of the free fragment. The final products will thus not absorb the probe wavelength, but instead the transition-states of the reaction may do so. The FTS transient will therefore be expected to build up, as the molecules enter the optically coupled region of the probe, and then subsequently decay, as the molecules move on to final products (see Fig. 3). By obtaining FTS transients for various values of λ_2^*, information on the shapes of the PES's involved can be obtained.

There are several points to be made regarding this reaction. First, the PES of ICN dissociation is more complex than the one illustrated in Fig. 1 because there are two channels (with possible crossings) for dissociation involving the production of iodine either in its ground or its excited spin-orbit states (Fig. 4). However, at 306 nm our available energy is just below the excited I* state channel, and it is known experimentally that at this excitation wavelength the reaction is to the ground state

channel, which correlates with a bent state. The measurements reported here clock the dynamics of I-CN recoil and the development of free CN. As pointed out by the groups of Zare, Wittig, Houston, and others, the dynamics that produce rotational excitation are due to bending, and could be on a shorter time scale. Time-resolved alignment experiments (discussed below) should aid us in resolving this bending dynamics. Second, the absorption measurement depends also on the characteristics of the upper state (I + CN*) potential. However, in the asymptotic limit ($R \rightarrow \infty$), $\tau_{\frac{1}{2}}$ is described by a simple formula (see publications), and as discussed below the shape of the transients, the direction of the probe wavelength shifts, and the effect of tuning the pump wavelength can separate V_1 and V_2 dynamics. Finally, we assumed here a repulsive potential, but there exists a method (R. Bernstein and A. Zewail, J. Chem. Phys. in press) to invert the data to give the shape of the PES and to account for the attractive terms in the potential.

Theoretically, these observations are reproduced using classical mechanical as well as quantum mechanical treatment of the dissociation. Even kinetics can describe the general behavior of the transients as detailed in the publications by Rosker *et al.* (see below). From these results we determine that the transition states en route to dissociation live for only 50-20 fs, depending on the R-region probed.

The new finding of the research done in these areas of femtosecond reaction dynamics are discussed in the following publications, following the initial work in 1985 [N. F. Scherer, J. L. Knee, D. D. Smith, and A. H. Zewail, *J. Phys. Chem.* 89, 5141 (1985)]:

1. Picosecond and Femtosecond Molecular Beam Chemistry: Coherence and Fragment Recoil Dynamics.
   Ahmed H. Zewail
   in: Ultrafast Phenomena V, Springer Series in Chemical Physics 46, eds. G. R. Fleming and A. E. Siegman (Springer-Verlag, 1986) p. 356.

2. Real-Time Femtosecond Probing of "Transition States" in Chemical Reactions.
   Marcos Dantus, Mark J. Rosker, and Ahmed H. Zewail
   J. Chem. Phys. 87, 2395 (1987)

3. Picosecond MPI Mass-Spectrometry of CH_3I in the Process of Dissociation.
   Lutfur R. Khundkar and Ahmed H. Zewail
   Chem. Phys. Lett. 142, 426 (1987)

4. Femtosecond Clocking of the Chemical Bond
   Mark J. Rosker, Marcos Dantus, and Ahmed H. Zewail
   Science 241, 1200 (1988)

5. Femtosecond Spectroscopy of Transition States in Reactions
   Ahmed H. Zewail

in: Springer Series in Chemical Physics 48, eds. T. Yajima, K. Yoshihara, C. B. Harris, S. Shionoya (Springer-Verlag, 1988) p. 500

6. Femtosecond Real-Time Probing of Reactions: I. The Technique.
Mark J. Rosker, Marcos Dantus, and Ahmed H. Zewail
J. Chem. Phys. 89, 6113 (1988)

7. Femtosecond Real-Time Probing of Reactions: II. The Dissociation of Reaction of ICN.
Marcos Dantus, Mark J. Rosker, and Ahmed H. Zewail
J. Chem. Phys. 89, 6128 (1988)

C. Theoretical Studies

To relate these FTS measurements to a dissociation time and to the characteristics of the PES, we first considered simple potentials of the form:

$$V(R,\theta) = V_0 \exp(-R/L_1)\, f(R,\theta),$$

where L_1 is the repulsion length parameter between fragments and $f(R,\theta)$ describes the angular part. The classical equation of motion for this system, without $f(R,\theta)$, can be integrated to give analytically the internuclear separation of the fragments as a function of time, R(t), and the corresponding potential as a function of time, V(t).

We then ask, what defines a dissociation time? If it were defined as the time for the two fragments to reach a separation at which their interaction energy is negligible, the dissociation time would depend on the sensitivity with which the energy can be measured; an infinite time is required to reach infinite separation. A more *invariant* definition is obtained as follows: Consider the difference between the time taken for the fragments to separate from R_0, the separation at the instant of photoexcitation, to R (as they travel along the actual potential) minus the time which would be required had the fragments traveled at the terminal velocity (v). Then τ_d is defined as the limit of this difference as $R \to \infty$. For the potential described above (with no anisotropy), one obtains: $\tau_d = (L_1/v)\, \ell n 4$. While well-defined, this τ_d is obtainable only from a hypothetical experiment requiring the measurement of minute differences in long arrival times (see Fig. 5).

A more useful description of bond breaking has been recently developed (R. Bersohn and A. Zewail) to consider the time dependence of fragment separation and the absorption by fragments during this separation. When the fragments develop to be spectroscopically free, the absorption achieves a maximum. Dissociation can be defined as the time delay when the mid-point of the absorption is reached:

$$\tau_{1/2} = (L_1/v)\, \ell n\, (4E/\gamma).$$

Here, γ is the half-width of the energy distribution of the probe pulse, and E is the energy available above dissociation ($E \gg \gamma$). An important observation is contained within this analysis: the probe spectral width determines a "window" through which the free fragment (e.g., CN) is viewed, and so affects $\tau_{1/2}$. Since we have both γ and E the above expression yields for the repulsion length parameter L_1 = 0.8Å, for the exponential potential discussed above. A similar procedure can be used to calculate length parameters of other potential shapes, e.g., R^{-n}. According to the above analysis, the potential falls to 1/e of its initial value in 0.8Å, but the distance corresponding to $\tau_{1/2}$ (the time taken for the potential to drop to γ) is 4Å. This classical mechanical description reproduces the experimental observations, as shown in Fig. 6, and compares well with recent quantum mechanical calculations (Fig. 7).

The above analysis assumes a potential and derives the parameters of this potential from the data. More recently we (R. Bernstein and A. Zewail) developed a procedure for inverting the experimental data and obtaining the PES. Such an inversion is accomplished without prior knowledge of the shape of the PES (Fig. 8).

Quantum mechanically the time evolution of fragment separation can be described and in the case of ICN, a wave packet approach has been used by D. Imre (Fig. 7) to reproduce the experimental observations. The agreement between the quantum calculations and the classical mechanical model is remarkable in that both show the expected FTS of ICN on-resonance (free fragment detection) and off-resonance.

These theoretical studies of the FTS experiments have also been extended to other reactions (to be discussed below) and the major findings are summarized in the following publications:

1. Time Dependent Absorption of Fragments During Dissociation.
   R. Bersohn and A. H. Zewail
   Ber. Bunsenges. Phys. Chem. 92, 373 (1988)

2. Femtosecond Real-Time Probing of Reactions: I. The Technique.
   Mark J. Rosker, Marcos Dantus, and Ahmed H. Zewail
   J. Chem. Phys. 89, 6113 (1988)

3. Femtosecond Real-Time Probing of Reactions: II. The Dissociation of Reaction of ICN.
   Marcos Dantus, Mark J. Rosker, and Ahmed H. Zewail
   J. Chem. Phys. 89, 6128 (1988)

4. Femtosecond Real-Time Probing of Reactions: III. Inversion to the Potential from Femtosecond Transition-State Spectroscopy Experiments.

Richard B. Bernstein and Ahmed H. Zewail
J. Chem. Phys. 90, 829 (1989)

5. Molecular State Evolution After Excitation with an Ultra-Short Laser Pulse: A Quantum Analysis of NaI and NaBr Dissociation.
Volker Engel, Horia Metiu, Raphael Almeida, R. A. Marcus and Ahmed H. Zewail
Chem. Phys. Lett. 152, 1 (1988)

D. Extension to "Oriented" Bimolecular Reactions

An important new issue arises for bimolecular reactions that is not a concern in the unimolecular case. For a unimolecular reaction, the reaction begins ($t=0$) when the laser pulse initiates excitation and subsequent dissociation. But for a bimolecular reaction, whether in bulk or in crossed beams, there is no comparable way to establish the beginning point for the reaction.

However, for a special class of reactions one can establish the zero of time within an uncertainty governed by the laser pulse duration only. This has now made it possible to study real-time dynamics of these bimolecular reactions. The first of these experiments by Scherer *et al.* has been conducted in the picosecond, rather than femtosecond, time domain, but the principle is the same. The method involves the use of a beam of a van der Waals "precursor molecule" containing the potential reagents in close proximity. Here, we make use of the approach of weak molecular complexes, as pioneered by Wittig's and Soep's groups to study product-state distributions, so we can establish the zero of time and hence follow the course of the reaction in real time. For the reaction studied,

$$H + OCO \rightarrow [HOCO]^{\ddagger} \rightarrow OH + CO,$$

the precursor molecule was IH ··· OCO, formed in a free-jet expansion of a mixture of HI and CO_2 in an excess of helium carrier gas. Such van der Waals complexes have favorable geometry which limits the range of impact parameters and angles of attack of the H on the OCO.

To clock the reaction, an ultrashort laser pulse initiates the experiment by photodissociating the HI, ejecting a translationally hot H atom in the general direction of the nearest neighbor O atom in the CO_2. A probe laser pulse tuned to a wavelength suitable for detection of the OH was delayed relative to the photolysis pulse using a Michelson interferometer. The OH appeared after a delay of a few picoseconds from the initiation pulse. This delay represents a direct measure of the lifetime of the $[HOCO]^{\ddagger}$ collision complex at the available energy of the collision (Fig. 9). The lifetime changes with translational energy.

As discussed below, a new series of experiments using femtosecond pulses is needed in order to follow the formation and decay of the collision complex in the femtosecond region, and to study the effect of limited impact parameter (orientation), an important feature of this approach, on the reaction dynamics. Comparison with classical trajectory calculations, based upon the *ab initio* calculated PES, will be important. The following summarizes the results of our efforts in this direction:

1. Real-Time Picosecond Clocking of the Collision Complex in a Bimolecular Reaction: The Birth of OH from H + CO_2.
   Norbert F. Scherer, Lutfur R. Khundkar, Richard B. Bernstein, and Ahmed H. Zewail
   J. Chem. Phys. 87, 1451 (1987)

2. Real-Time Picosecond Clocking of "oriented" Bimolecular Reactions: The IH ... OCO System.
   N. F. Scherer, C. Sipes, R. B. Bernstein, and A. H. Zewail-
   to be published

E. Reactions of alkali halides: Covalent to Ionic Crossings

For direct dissociation reactions, the molecules are in "transition" for only fifty femtoseconds or so, as evidenced by the rise and decay observed in the ICN experiments and confirmed by theory. If, however, in the process of falling apart, the system encounters a well in the potential surface, or if there is more than one degree of freedom involved, the system can be "trapped" and thus exhibit behavior indicative of quasi-bound states, or resonances. In real time, manifestation of these resonances would be a slow down in the appearance of free fragments and possibly the appearance of oscillations reflecting the vibrational resonance frequency of the wave packet of the dissociating fragments.

The classic reactions of alkali metal-halogen are prototype systems for such studies. This class of reactions has been studied before in the "alkali age" of molecular beam scattering of alkali metal (M) and halogen (X). And, observing their real-time behavior will be of great interest. Because of the ionization potential of M and the electron affinity of X, the energy of $M^+ + X^-$ is higher than that of M + X. In the ground state the molecule is ionic M^+X^- and this state correlates with the $M^+ + X^-$ (see Fig. 10). Hence, the covalent potential curve (M + X) crosses the ionic (Coulombic) curve. Because of this crossing (or avoided crossing) at certain M ··· X separation (R_x), electron harpooning takes place. The potential energy surfaces for such important processes have been described in a classic series of papers by Berry.

In the femtosecond experiments conducted in this laboratory, the initial pulse at λ_1 takes the molecule from the M^+X^- ground state to the covalent surface MX*. The second pulse probes the reaction at λ_2^* (transition-state region) and at λ_2^∞ (final product; in this case Na):

$$MX^* \rightarrow [M\cdots X]^{\ddagger *} \rightarrow M + X \qquad (M = Na : X = I,Br)$$

En route to products, the $[M\cdots X]^{\ddagger *}$ transition state molecules "decide" between ionic and covalent paths; either the packet of MX* will be trapped on the adiabatic potential curve or it will dissociate by following the diabatic curve. The two cases have entirely different temporal behavior and, if there is trapping, the frequency and amplitude of the oscillations will provide details of the nature of the surfaces and the strength of the coupling. Comparison with the theory of Grice and Herschbach and others can then be made.

The experiments show (Fig. 11) a striking oscillatory behavior (when probing at λ_2^*) that persists for picoseconds (~ 10 oscillations) in the case of NaI, and for less time (~ 2 oscillations) for the NaBr case. Probing on-resonance (at λ_2^∞) gives a rise with plateaus separated by the same oscillation frequency. This on-resonance "integration" of the trajectories is a clear demonstration of the concept of FTS, discussed earlier. The average period for NaI reaction is 1.25 ps, which corresponds to a frequency of 27 cm^{-1}. It is concluded that the packet for NaI is effectively trapped in the adiabatic well en route to products, and that the observed oscillations represent "pulses of Na atoms" leaving the well. Since the oscillation damping time for NaI is ~ 10 ps, one crossing on the outward phase per oscillation (~ 1 ps) has a probability of about 0.1 to escape from the well. For NaBr, the frequency of oscillation is similar in magnitude, but severe damping is observed. Thus, the crossing for NaBr is much more facile than for NaI, consistent with theoretical expectation. In the references given below we compared theory with experiments and obtained the Landau-Zener probability of escape, the anharmonicity of the PES, and the coupling between the covalent and ionic curves. An interesting question is how the "dephasing" and spread of the wave packet influences the dissociation rate, as determined by the decay of the oscillations. The experiments do show manifestations of this decay and spreading, and theoretical modeling of the wave packet dynamics in these prototype systems is important. Very recently, quantum and semiclassical calculations (Fig. 12) have been performed (in collaboration with H. Metiu and R. Marcus) and agreement with the experiment is good. When these experiments are completed we will be able to make contact with other spectroscopic findings (absorption, scattering, photofragmentation) and with recent wing emission studies

by the Polanyi group. Our goal is to understand wave packet dynamics in these prototype systems and deduce characteristics of the PES. The new finding are given in the following publications:

1. Femtosecond Real-Time Observation of Wave Packet Oscillations (Resonance) in Dissociation Reactions.
   Todd S. Rose, Mark J. Rosker, and Ahmed H. Zewail
   J. Chem. Phys. 88, 6672 (1988)

2. Femtosecond Real-Time Dynamics of Photofragment-Trapping Resonances on Dissociative Potential Energy Surfaces.
   Mark J. Rosker, Todd S. Rose, and Ahmed H. Zewail
   Chem. Phys. Lett. 146, 175 (1988)

3. Molecular State Evolution After Excitation with an Ultra-Short Laser Pulse: A Quantum Analysis of NaI and NaBr Dissociation.
   Volker Engel, Horia Metiu, Raphael Almeida, R. A. Marcus, and Ahmed H. Zewail
   Chem. Phys. Lett. 152, 1 (1988)

F. General Reports

In several review articles from this group, or in collaboration with other colleagues, the above results and their general implications have been discussed:

1. Laser Femtochemistry.
   Ahmed H. Zewail
   Science 242, 1645 (1988)

2. Femtochemistry: The Role of Alignment and Orientation.
   Ahmed H. Zewail
   J. Chem. Soc., Faraday Trans. 2, 85 (1989)

3. Femtosecond Spectroscopy of Transition States in Reactions.
   Ahmed H. Zewail
   in: Ultrafast Phenomena VI, Springer Series in Chemical Physics 48
   eds: T. Yajima, K. Joshihara, C. B. Harris, and S. Shionoya
   (Springer-Verlag, 1988) p. 500

4. Real-Time Laser Femtochemistry: Viewing the Transition States from Reagents to Products.
   Ahmed H. Zewail and Richard B. Bernstein
   Chemical & Engineering News (Feature Article/Special Report)
   November 7, 1988, p. 24-43

5. Ultrafast Laser Spectroscopy of Chemical Reactions.
   Joseph L. Knee and Ahmed H. Zewail
   Spectroscopy (invited article) 3, 44 (1988)

6. Real-Time Femtochemistry.
   A. H. Zewail and R. B. Bernstein
   Kagaku to Kogyo (Chemistry and Chemical Industry) 41, 108 (198

Over the past three years we have been very fortunate in developing femtochemistry, and we hope that in the coming three years new areas of studies will be conducted to map out the dynamics of elementary reactions in real time.

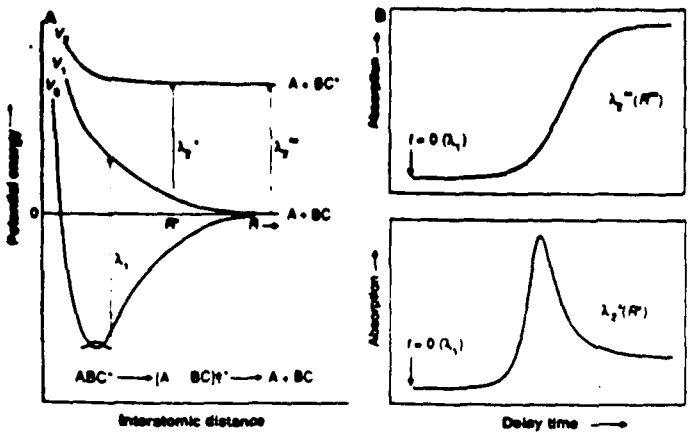

Fig. 3. The concept of observing the transition region of a reaction and the idea of an FTS experiment. (**A**) The potential energy curves are for a bound molecule (V_0), and for the first and second dissociative curves, V_1 and V_2. The repulsion between fragments on V_1 and V_2 leads to bond breaking. The pump femtosecond pulse (λ_1) takes the molecule from V_0 to V_1. As the fragments recoil, the pulse at λ_2^* (or λ_2^∞) probes the transition region (or the free fragments). (**B**) The expected femtosecond transients, signal versus delay time between pump and probe pulses, at λ_2^* and λ_2^∞.

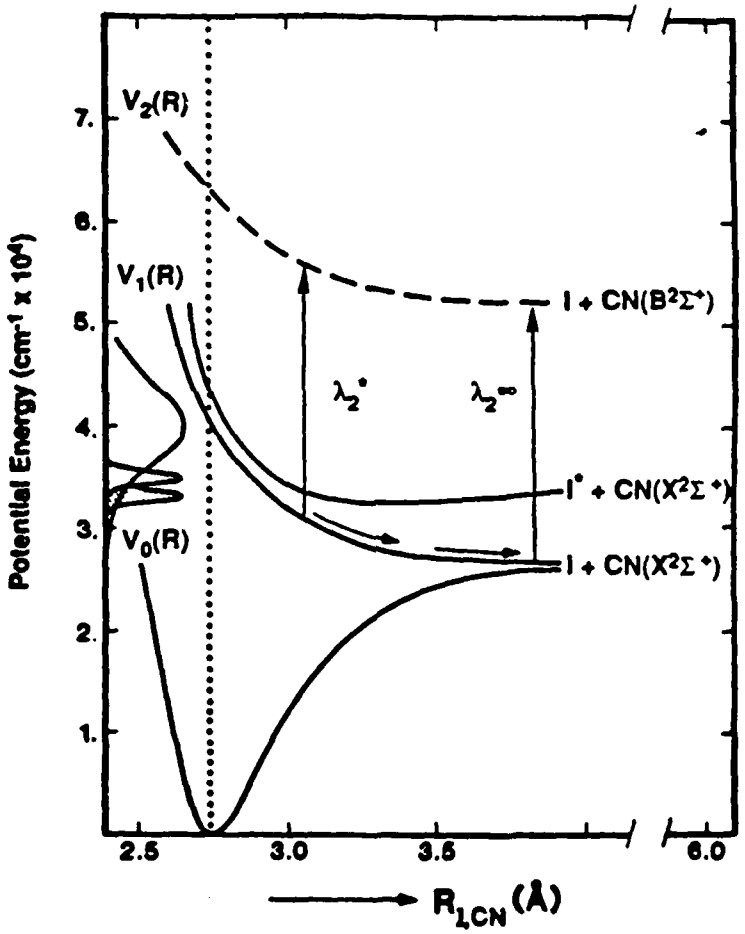

Fig 4: PES for ICN dissociation

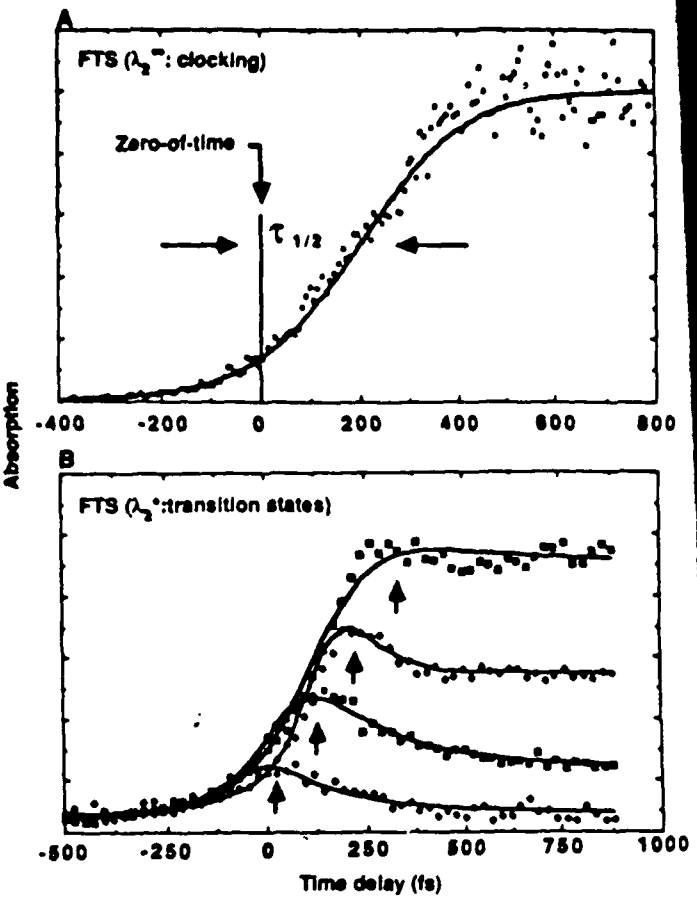

Fig. 2. FTS results for the reaction $ICN^* \rightarrow [I \cdots CN]^* \rightarrow I + CN$. (**A**) The delayed appearance of free CN fragments (by 205 ± 30 fs) was probed at λ_2^∞ (388.5 nm). In these experiments the zero-of-time was established to determine the bond-breaking time $\tau_{1/2}$. (**B**) Transients taken for different λ_2^* probings to the red wavelengths (389.7, 389.8, 390.4, and 391.4 nm) of absorption by free fragments. Note that as tuning is increased more to the red, the absorption maximum shifts to earlier times, as expected (see text).

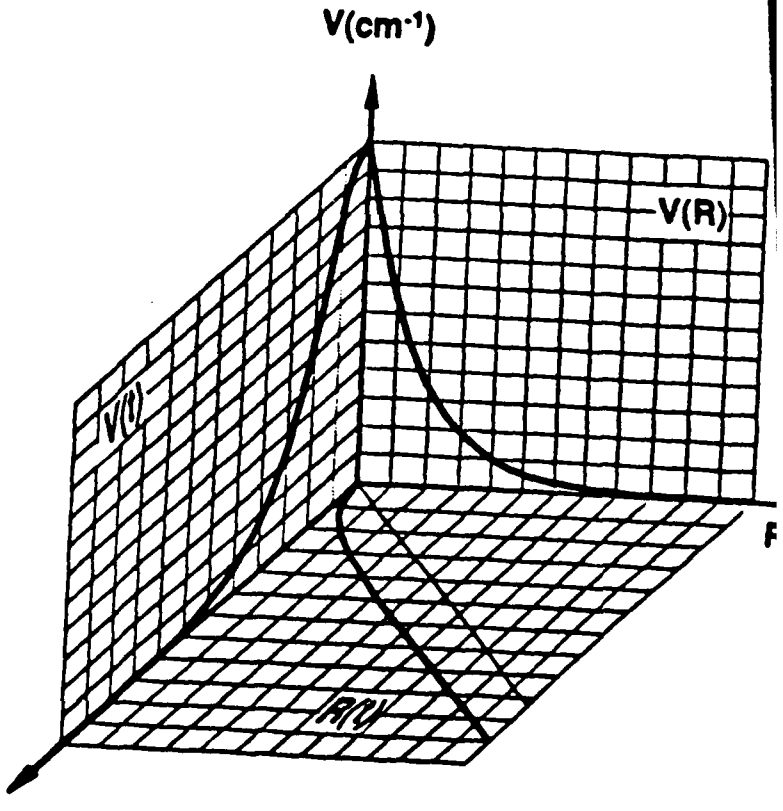

Fig 5: The potential energy curves V(R), V(t), and R(t) for

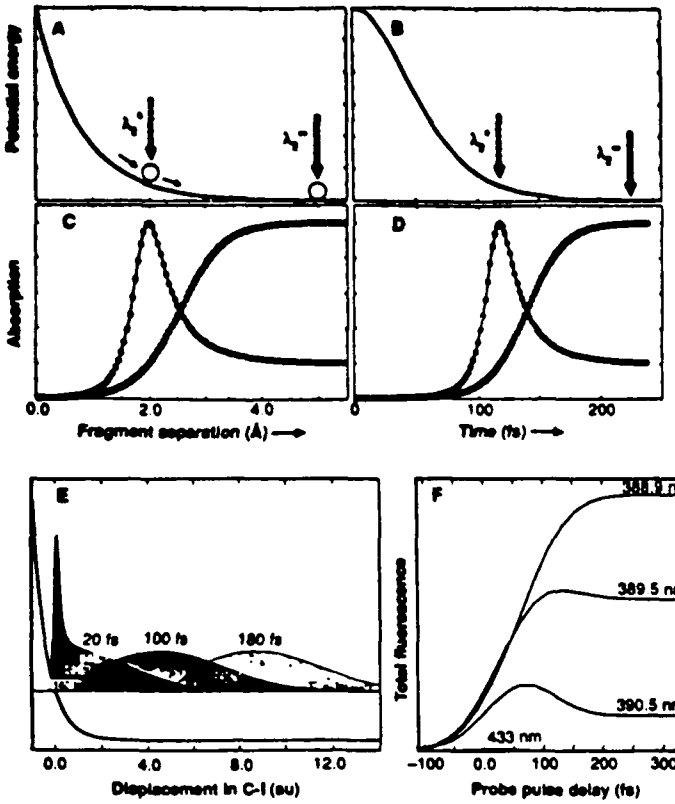

Fig 6.7 (A through D) Theoretical classical-mechanics calculations for the reaction $ICN^* \rightarrow [I \cdots CN]^{\ddagger *} \rightarrow I + CN$. The potential energy as a function of (A) fragment separation $[V(R)]$ and (B) time $[V(t)]$. By 200 fs, the bond is essentially broken. The probing at λ_2^* and λ_2^∞ is depicted on the PES, and the calculated FTS signals are shown at these two wavelengths of probing as a function of (C) fragment separation $[A(R)]$ and (D) time $[A(t)]$ ($\gamma = 250\ cm^{-1}$, and $L = 0.8$ Å). This simple theory reproduces the major features of the experiments (see text). (E and F) Theoretical quantum mechanical calculations for the same reaction. (E) The wave packet propagation with time, executing ~5 Å in 200 fs. (F) The expected FTS signal is shown and again reproduces the experimental observations

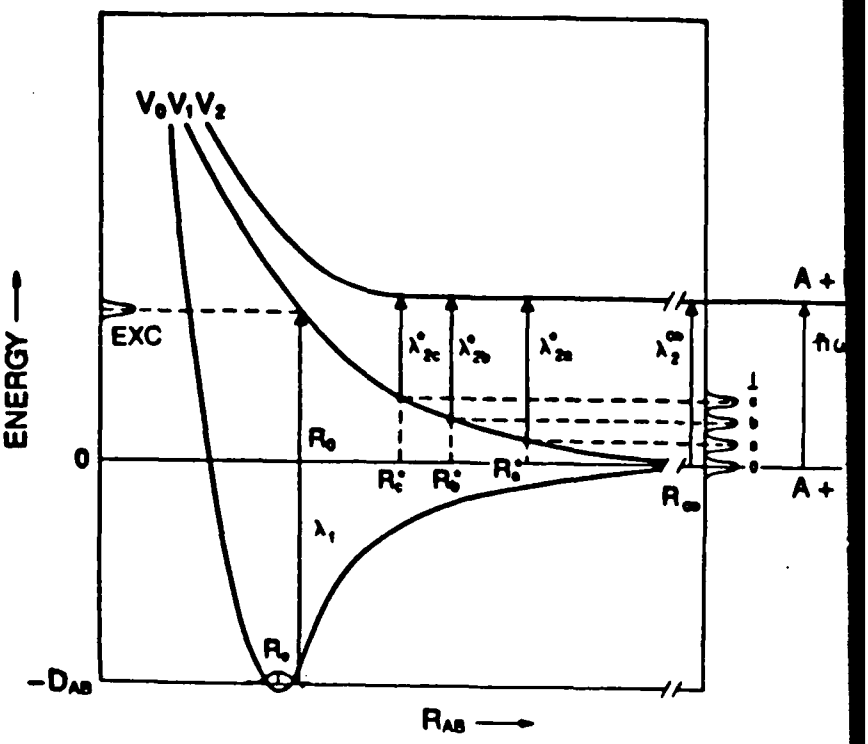

Fig 8a: The PES and the idea of the inversion method for different probings at λ_2^*.

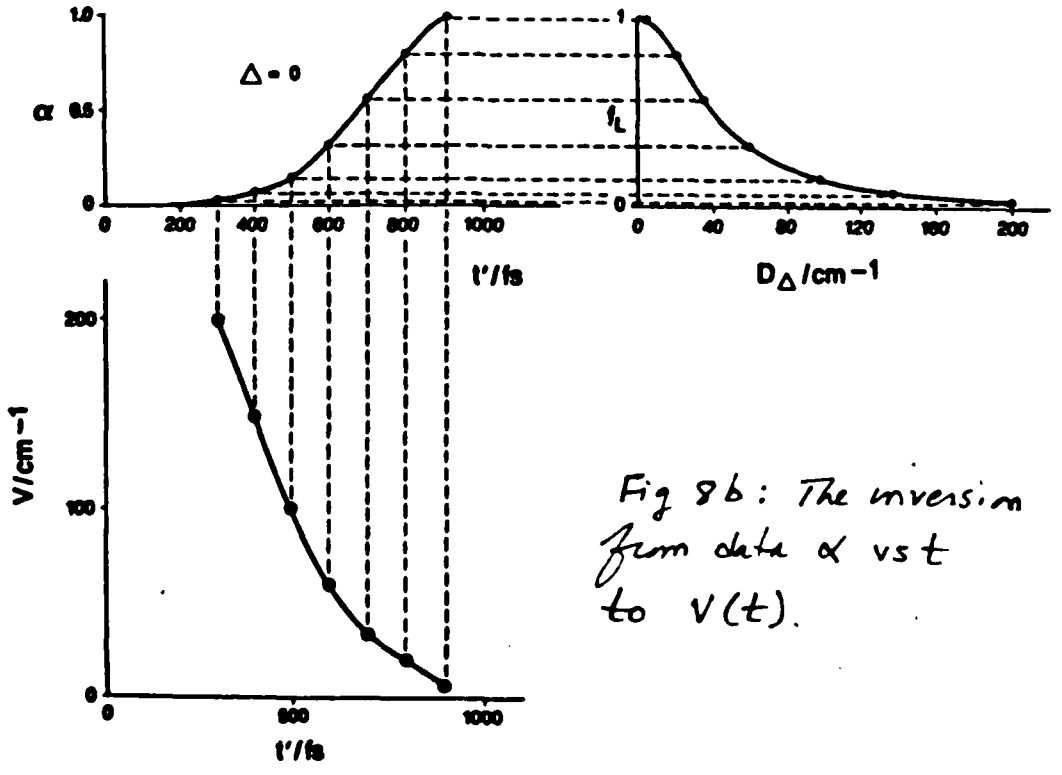

Fig 8b: The inversion from data α vs t to V(t).

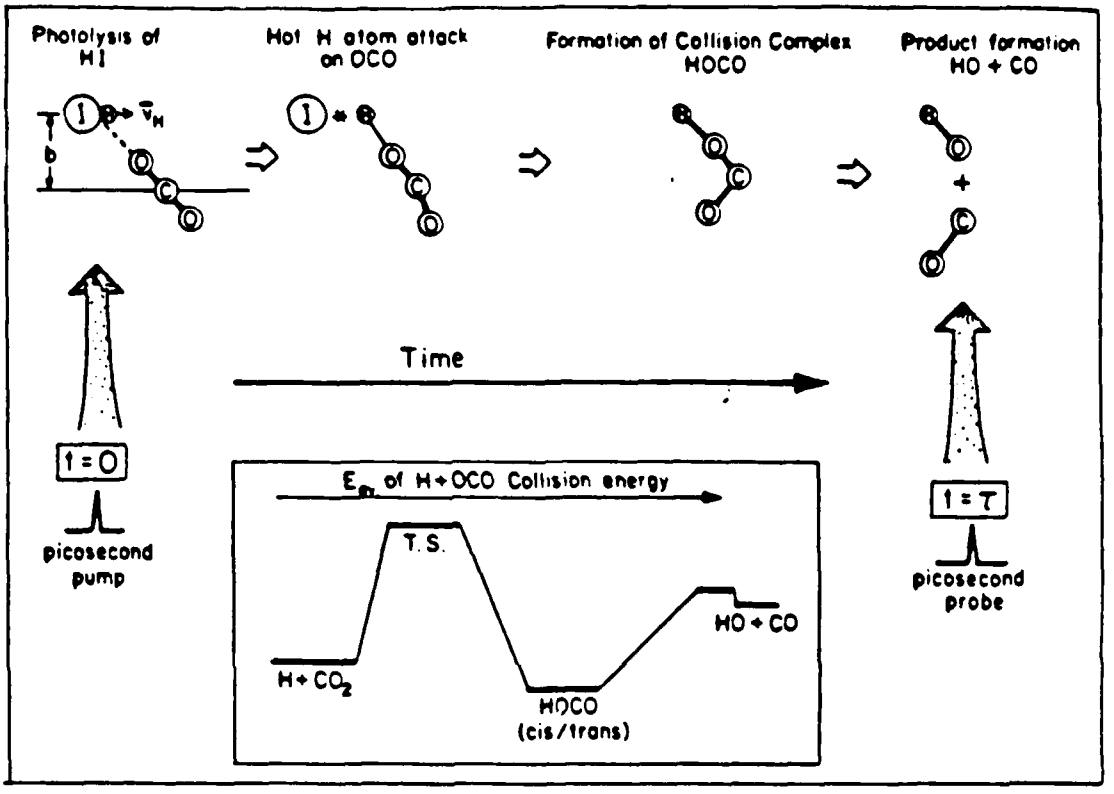

Fig 9a : schematic of the pump-probe experiment on "oriented" bimolecular reactions.

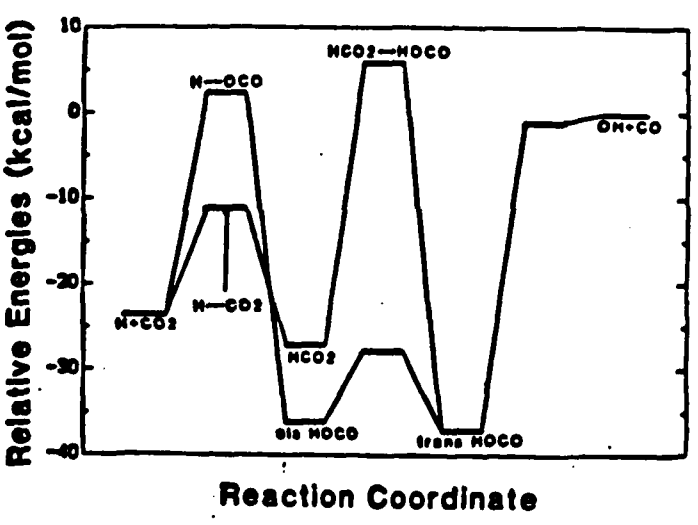

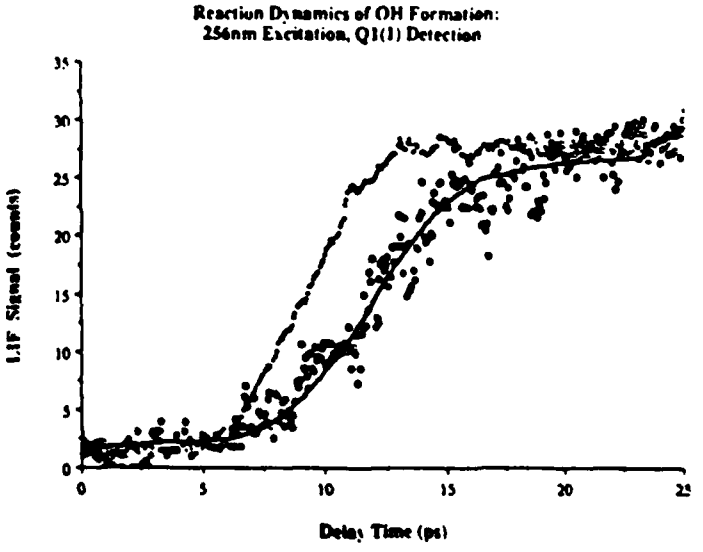

Fig 9b: The PES and the observed transients.

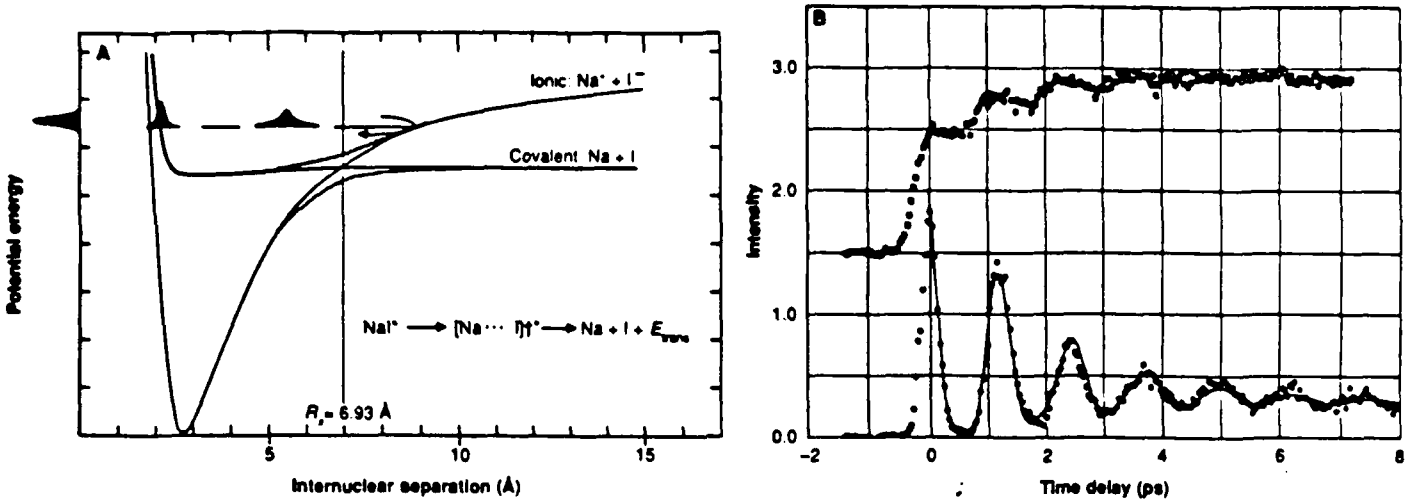

Fig. 10. Potential energy curves for reactions of alkali halides displaying the ionic and covalent states of the reaction. The pump pulse (λ_1), indicated by the bell-shaped curve on the vertical axis, takes the salt Na^+I^- to the covalent surface NaI*. As the bond stretches $[Na\cdots I]^{\ddagger *}$, the probe ($\lambda_2$) monitors the evolution of the wave packet (indicated by the bell-shaped curve moving along R) of dissociating molecules in the transition region (λ_2^*) and at "infinite" separation (λ_2^∞). Note the avoided crossing between the ionic and covalent curves and the possible trapping of the packet that may result from this electron harpooning at the crossing point, R_x (see text). (**B**) FTS experimental results for the reaction of alkali halides $NaI^* \rightarrow [Na\cdots I]^{\ddagger *} \rightarrow Na + I$. The transient at the bottom shows the oscillatory (resonance) behavior of the wave packet as it moves back and forth between the covalent and ionic curves of (A). Each time the packet comes near the crossing point there is a probability of escape (~0.1), which is observed as a damping of the oscillations. The resonance frequency gives the round trip time in the well. The experiment was performed by exciting at 310 nm and detecting off-resonance to the transition of free Na atom at 589 nm. When detecting on-resonance, the transient at the top was obtained. On-resonance, the trajectory is "integrated" over the entire distance and one expects an integration of the oscillation to yield plateaus, with steps given exactly by the resonance frequency, as observed experimentally. This result is a clear demonstration of the idea of FTS (see text).

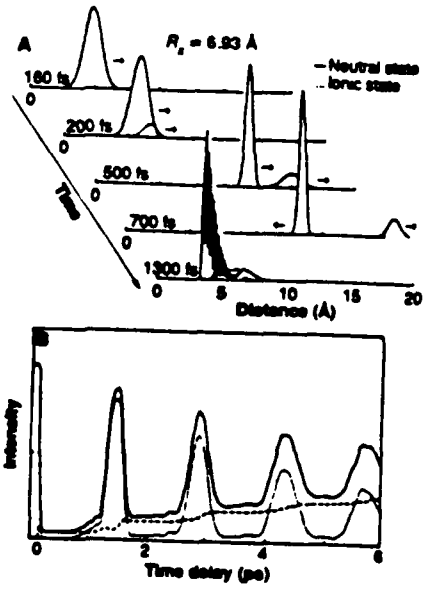

Fig. 12. Theoretical quantum-mechanical calculations of the reaction of NaI. (**A**) Snapshots of the wave packet as it propagates from the initial covalent configuration, before and after the crossing point (see Fig. 7A). Note the "splitting" of the packet to neutral (solid line) and ionic (dotted line) states as a function of time. These are typical results for the different λ_1s studied. (**B**) The expected FTS transient (at λ_1 = 300 nm) when detecting free fragment [(λ_2^∞), steps with plateaus] and in the transition region [(λ_2^*), oscillatory behavior]. The solid line is the total signal. The calculations are consistent with experiments and with the derived parameters obtained by the experiments. The calculations are given in (44) by Engel *et al.* (See text)

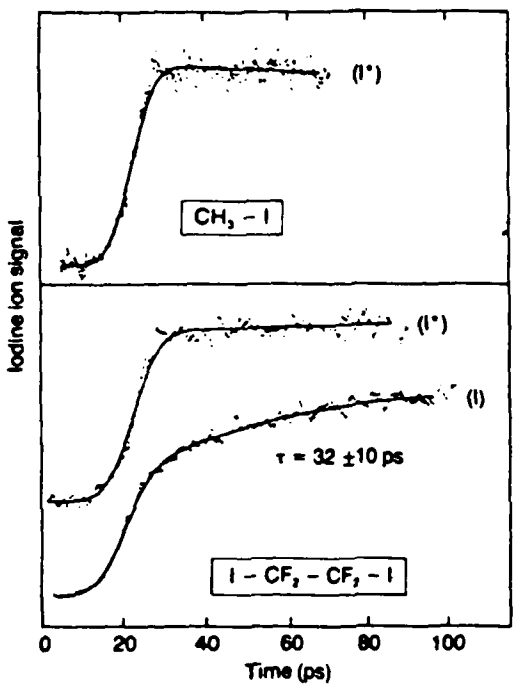

Figure 13 Product-I atom multiphoton ionization signal as a function of pump–probe delay time. The top trace is the unresolved dissociation of methyl iodide, in this case detecting the I* state ($^2P_{1/2}$). The second transient is a similar result for $C_2F_4I_2$ and is contrasted to the slower rising transient appearance of I ($^2P_{3/2}$) atoms. These I($^2P_{3/2}$) atoms result from the secondary reaction, $C_2F_4I \rightarrow C_2F_4 + I$.

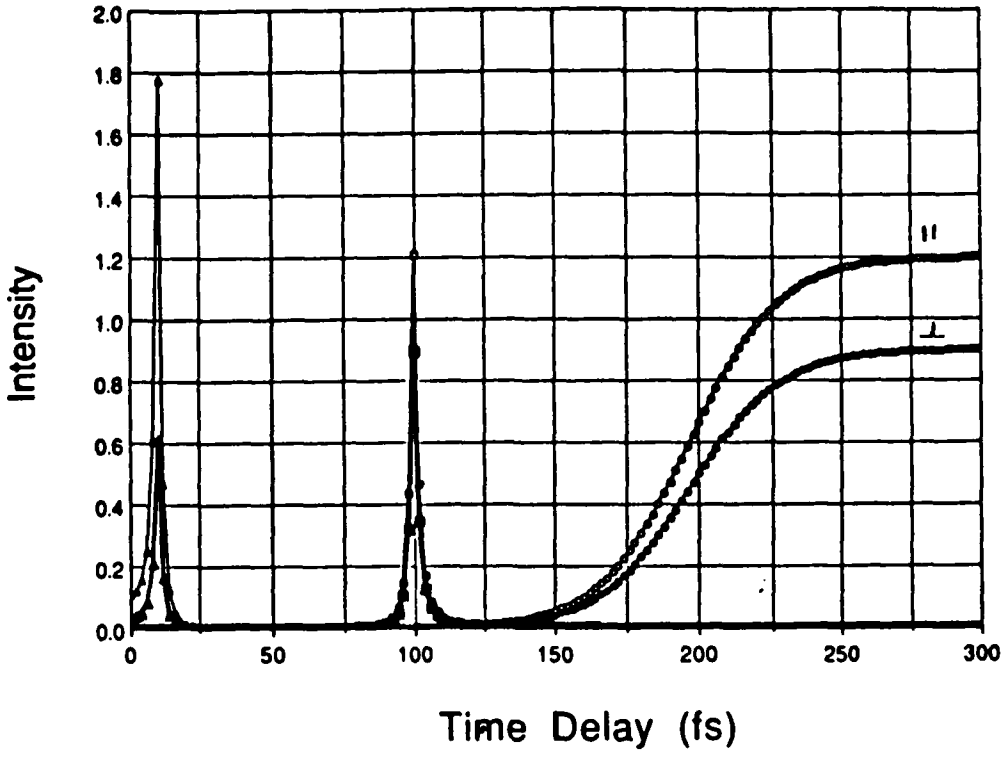

Fig 14: I_{II} and $I_{\perp}$ vs. t in fS. Note the large anisotropy at early times, which relates directly to the torque (see text).

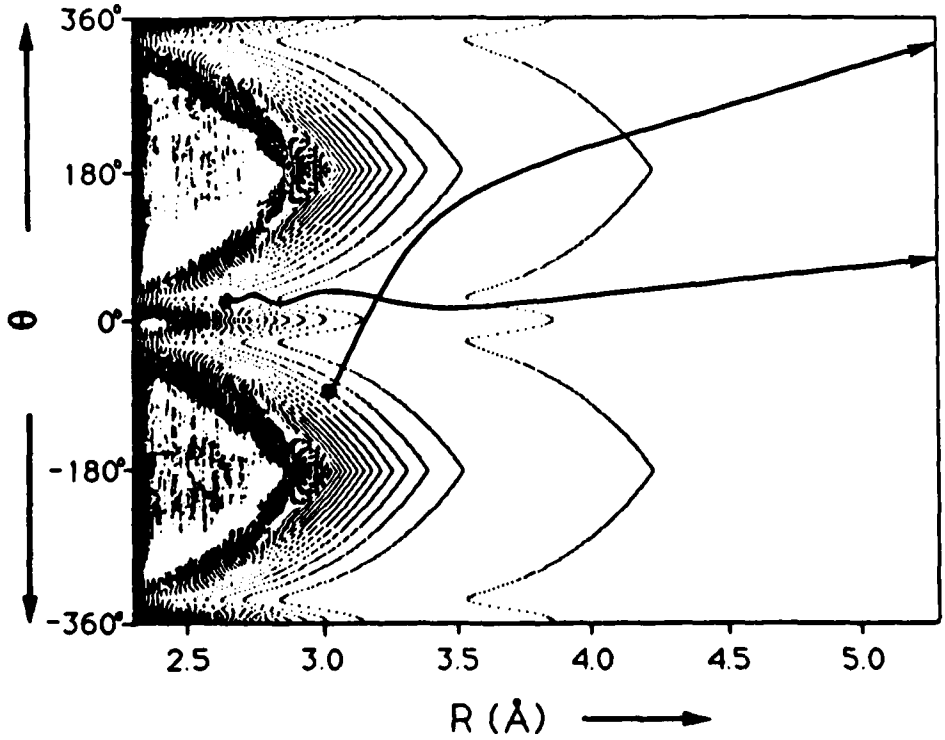

Fig 15: Different trajectories of dissociation (ICN) starting from a linear and bent configuration. Note the different $T_{\perp}$'s (dark)